

Mass and pressure constraints on galaxy clusters from interferometric SZ observations

Malak Olamaie,^{1*} Michael P. Hobson¹ and Keith J. B. Grainge^{1,2}

¹ *Astrophysics Group, Cavendish Laboratory, 19 J. J. Thomson Avenue, Cambridge, CB3 0HE*

² *Kavli Institute for Cosmology Cambridge, Madingley Road, Cambridge, CB3 0HA*

Accepted ??????; Received ???????

ABSTRACT

Following on our previous study of an analytic parametric model to describe the baryonic and dark matter distributions in clusters of galaxies with spherical symmetry, we perform an SZ analysis of a set of simulated clusters and present their mass and pressure profiles. The simulated clusters span a wide range in mass, $2 \times 10^{14} M_{\odot} < M_{\text{tot}}(r_{200}) < 1.0 \times 10^{15} M_{\odot}$, and observations with the Arcminute Microkelvin Imager (AMI) are simulated through their Sunyaev-Zel'dovich (SZ) effect. We assume that the dark matter density follows a Navarro, Frenk and White (NFW) profile and that the gas pressure is described by a generalised NFW (GNFW) profile. By numerically exploring the probability distributions of the cluster parameters given simulated interferometric SZ data in the context of Bayesian methods, we investigate the capability of this model and analysis technique to return the simulated clusters input quantities. We show that considering the mass and redshift dependency of the cluster halo concentration parameter is crucial in obtaining an unbiased cluster mass estimate and hence deriving the radial profiles of the enclosed total mass and the gas pressure out to r_{200} .

Key words: galaxies: clusters– cosmology: observations – methods: data analysis

1 INTRODUCTION

Determining the properties of clusters of galaxies such as their total and baryonic mass offers an independent and powerful cosmological tool to constrain the parameters of the Λ CDM model. The mass distribution of clusters is usually measured using a variety of observational methods, including X-ray, Sunyaev–Zeldovich (SZ) (Sunyaev & Zeldovich 1970; Birkinshaw 1999; Calstrom, Holder & Reese 2002), and gravitational lensing analyses. These methods are often based on parameterised cluster models for the distribution of the cluster dark matter and the thermodynamical properties of its intra-cluster medium (ICM). However, these various approaches usually lead to different estimates of the cluster mass. This is due to either extrapolating to halo masses and to redshifts that are not well sampled by the data or fitting for model parameters to which the data are insensitive.

In this letter, we perform a detailed analysis of a sample of nine simulated SZ observations of galaxy clusters in a mass range of $2 \times 10^{14} M_{\odot} < M_{\text{tot}}(r_{200}) < 1.0 \times 10^{15} M_{\odot}$ at redshift $z = 0.3$ as if observed with Arcminute Microkelvin Imager (AMI) (AMI Consortium: Zwart et al. 2008). To study the cluster total mass, we use the model described in Olamaie et al. (2012), which has the following main characteristic features: (1) host halo density profile follows a Navarro, Frenk and White (NFW) (Navarro et al. 1997) profile and the gas pressure is described by a generalised

NFW (GNFW) profile (Nagai et al. 2007) with fixed shape parameters, both in accordance with numerical simulations; (2) the gas distribution is in hydrostatic equilibrium with the cluster total gravitational potential dominated by dark matter and both dark matter and gas are spherically symmetric; and (3) the local gas fraction is much less than unity throughout the cluster, i.e. $\frac{\rho_{\text{gas}}(r)}{\rho_{\text{tot}}(r)} \ll 1$ for all r . This final assumption allows us to write $\rho_{\text{tot}}(r) = \rho_{\text{DM}}(r) + \rho_{\text{gas}}(r) \approx \rho_{\text{DM}}(r)$. We show that assuming the dark matter halo concentration parameter as an independent free parameter in the analysis has the potential to introduce biases in the cluster mass estimate, and hence it is crucial to consider the mass and redshift dependency of this parameter in the analysis. Throughout, we assume a Λ CDM cosmology with $\Omega_{\text{M}} = 0.3$, $\Omega_{\Lambda} = 0.7$, $\sigma_8 = 0.8$, $h = 0.7$, $w_0 = -1$, $w_a = 0$.

2 MODELLING AND ANALYSIS OF SIMULATED INTERFEROMETRIC SZ OBSERVATIONS

As the SZ surface brightness is proportional to the line-of-sight integral of the pressure of the hot plasma in the ICM, SZ analysis of galaxy clusters provides a direct measurement of the pressure distribution of the ICM.

The observed SZ surface brightness in the direction of electron reservoir may be described as

$$\delta I_{\nu} = T_{\text{CMB}} y f(\nu) \left. \frac{\partial B_{\nu}}{\partial T} \right|_{T=T_{\text{CMB}}} . \quad (1)$$

* Email: mo323@mrao.cam.ac.uk

Here B_ν is the blackbody spectrum, $T_{\text{CMB}} = 2.73$ K (Fixsen et al. 1996) is the temperature of the CMB radiation, $f(\nu) = \left(x \frac{e^x + 1}{e^x - 1} - 4\right)(1 + \delta(x, T_e))$ is the frequency dependence of thermal SZ signal, $x = \frac{h_p \nu}{k_B T_{\text{CMB}}}$, h_p is Planck's constant, ν is the frequency and k_B is Boltzmann's constant. $\delta(x, T_e)$ takes into account the relativistic corrections due to the relativistic thermal electrons in the ICM and is derived by solving the Kompaneets equation up to the higher orders (Rephaeli 1995, Itoh et al. 1998, Nozawa et al. 1998, Pointecouteau et al. 1998 and Challinor and Lasenby 1998). It should be noted that at 15 GHz (AMI observing frequency) $x = 0.3$ and therefore the relativistic correction, as shown by Rephaeli (1995), is negligible for $k_B T_e \leq 15$ keV. The dimensionless parameter y , known as the Comptonization parameter, is the integral of the number of collisions multiplied by the mean fractional energy change of photons per collision, along the line of sight

$$y = \frac{\sigma_T}{m_e c^2} \int_{-\infty}^{+\infty} n_e(r) k_B T_e(r) dl = \frac{\sigma_T}{m_e c^2} \int_{-\infty}^{+\infty} P_e(r) dl, \quad (2)$$

where $n_e(r)$, $P_e(r)$ and T_e are the electron number density, pressure and temperature at radius r respectively. σ_T is Thomson scattering cross-section, m_e is the electron mass, c is the speed of light and dl is the line element along the line of sight. It should be noted that in equation (2) we have used the ideal gas equation of state.

Moreover, the integral of the Comptonization y parameter over the solid angle Ω subtended by the cluster (Y_{SZ}) is proportional to the volume integral of the gas pressure. It is thus a good estimate for the total thermal energy content of the cluster and hence its mass (see e.g. Bartlett & Silk 1994). The Y_{SZ} parameter in both cylindrical and spherical geometries may be described as

$$Y_{\text{cyl}}(R) = \frac{\sigma_T}{m_e c^2} \int_{-\infty}^{+\infty} dl \int_0^R P_e(r) 2\pi r ds, \quad (3)$$

$$Y_{\text{sph}}(r) = \frac{\sigma_T}{m_e c^2} \int_0^r P_e(r') 4\pi r'^2 dr', \quad (4)$$

where R is the projected radius of the cluster on the sky.

In this context we use the model described in Olamaie et al. (2012), with its corresponding assumptions on the dynamical state of the ICM, to model the SZ signal and determine the radial profiles of M_{tot} and P_e for nine simulated clusters. The model assumes that the dark matter density follows a Navarro, Frenk and White (NFW) profile (Navarro et al. 1997) and the ICM plasma pressure is described by the generalised NFW (GNFW) profile (Nagai et al. 2007),

$$\rho_{\text{DM}}(r) = \frac{\rho_s}{\left(\frac{r}{R_s}\right) \left(1 + \frac{r}{R_s}\right)^2}, \quad (5)$$

$$P_e(r) = \frac{P_{\text{ei}}}{\left(\frac{r}{r_p}\right)^c \left(1 + \left(\frac{r}{r_p}\right)^a\right)^{(b-c)/a}}, \quad (6)$$

where ρ_s is an overall normalisation coefficient, R_s is the scale radius where the logarithmic slope of the profile $\ln \rho(r)/\ln r = -2$, P_{ei} is also an overall normalisation coefficient of the pressure profile and r_p is the scale radius. It is common to define the latter in terms of r_{500} , the radius at which the mean enclosed density is 500 times the critical density at the cluster redshift, and the gas concentration parameter, $c_{500} = r_{500}/r_p$. The parameters (a, b, c) describe the slopes of the pressure profile at $r \approx r_p$, $r > r_p$ and $r \ll r_p$ respectively. In the simplest case, we follow Arnaud et al. (2010) and fix the values of the gas concentration parameter and the slopes to be $(c_{500}, a, b, c) = (1.156, 1.0620, 5.4807, 0.3292)$. It

is also common practice to define the halo concentration parameter, $c_{200} = \frac{r_{200}}{R_s}$, where r_{200} is the radius at which the enclosed mean density is 200 times the critical density at the cluster redshift. The cluster model parameters: ρ_s , R_s and P_{ei} and hence the pressure and the integrated mass distributions may be derived under the following assumptions: spherical symmetry; hydrostatic equilibrium; and that the local gas fraction is much less than unity, equations (3) to (11) in Olamaie et al. (2012). It should be noted that in Olamaie et al. (2012), we considered the halo concentration parameter, c_{200} as an input free parameter and studied the cluster profiles for a distribution of concentrations at a given mass and redshift. However, the results of our analysis showed that c_{200} remains unconstrained. c_{200} is a physical parameter, which reflects the background density of the Universe, and so is not a parameter that just defines the shape or the slope of the profile that can not be constrained by SZ only analysis of galaxy clusters. This therefore suggests that the concentration depends on the other physical sampling parameters for a given set of cosmological parameters, i.e., mass and redshift. Hence, in this letter, we consider such a dependency in our analysis and instead derive c_{200} .

We also note that The results of the studies on the relation between the structural properties of the dark matter halos such as concentration, spin and shape with mass and the redshift from both N -body simulations of cosmological structure formation in a Cold Dark Matter (CDM) Universe and observations of clusters of galaxies show a clear dependence of the concentration parameter on the halo mass and its redshift. This is based on the fact, as first discussed by Navarro, Frenk & White (1996) and (1997), that the concentration parameter reflects the background density of the Universe at its formation time and hence as small objects form first in a hierarchical universe, lower mass halos will be more concentrated than the massive ones (Navarro, Frenk & White 1997; Eke et al. 2001; Bullock et al. 2001; Pointecouteau et al. 2005; Macciò et al. 2007; Vikhlinin et al. 2006; Comerford et al. 2007; Salvador-Solé et al. 2007; Buote et al. 2007; Neto et al. 2007; Duffy et al. 2008; Mandelbaum et al. 2008; Rudd et al. 2008; Corless et al. 2009; Muñoz-Cuartas et al. 2011; Ettori et al. 2011; Bhattacharya et al. 2011). Moreover, all of these studies show that the concentration-mass relation is well fitted by a power law over the mass range $10^{11} - 10^{15} h^{-1} M_\odot$. However, studies on determining the normalisation coefficient and the slope of such relation are still ongoing, and in particular, cluster observations have yet to investigate this further. In this letter, we, therefore, decided to use the relation derived by Neto et al. (2007) from N -body simulation which has also been used by Corless et al. (2009) in their weak lensing analysis of three real clusters, namely

$$c_{200} = \frac{5.26}{1+z} \left(\frac{M_{\text{tot}}(r_{200})}{10^{14} h^{-1} M_\odot} \right)^{-0.1}. \quad (7)$$

We also studied the $c_{\text{vir}} - M_{\text{vir}}$ relation given by Muñoz-Cuartas et al. (2011) where the normalization coefficient and the slope vary with cosmic time. However, the results were the same as using equation (7) within our cluster halo mass range.

We generate a sample of nine simulated SZ clusters equally spaced in the mass range $2 \times 10^{14} M_\odot < M_{\text{tot}}(r_{200}) < 1.0 \times 10^{15} M_\odot$ using the above mentioned model, equation (7) and the input parameters $M_{\text{tot}}(r_{200})$, z and $f_{\text{gas}}(r_{200})$ listed in Tab. 1; this set of parameters fully describes the Comptonization y parameter. Further details of generating simulated SZ skies and observing them with a model AMI small array (SA) are described in Hobson & Maisinger (2002), Grainge et al. (2002), Feroz et al. (2009) and AMI Consortium: Olamaie et al. (2012).

Table 1. $M_{\text{tot}}(r_{200})$ used to generate simulated clusters and the thermal noise levels reached in the simulated observations of the cluster sample. Here σ_{SA} refers to the thermal noise levels reached in SA maps. All the clusters are generated at fixed redshift $z = 0.3$ and fixed $f_g(r_{200}) = 0.13$.

Cluster	$M_{\text{tot}}(r_{200}) 10^{14} M_{\odot}$	$\sigma_{\text{SA}} (\text{mJybeam}^{-1})$
clsim1	2.0	0.05
clsim2	3.0	0.06
clsim3	4.0	0.07
clsim4	5.0	0.06
clsim5	6.0	0.077
clsim6	7.0	0.08
clsim7	8.0	0.087
clsim8	9.0	0.07
clsim9	10.0	0.067

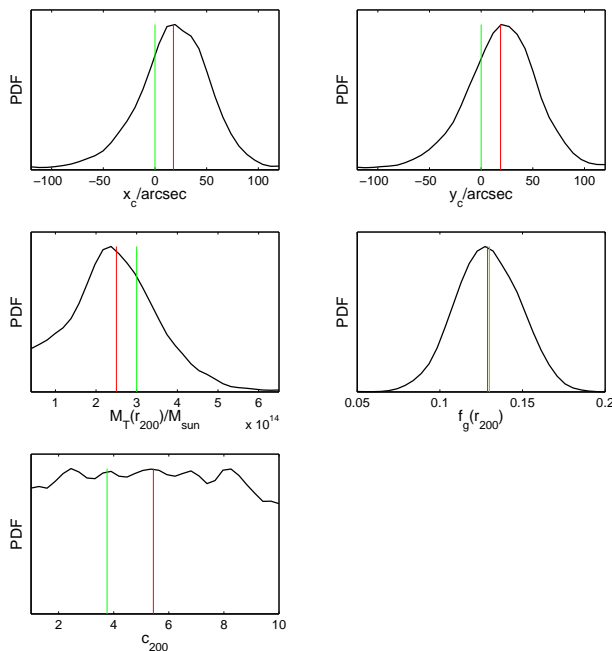


Figure 1. 1D marginalised posterior distributions of sampling parameters of clsim2 when c_{200} is also assumed to be an input parameter. Green vertical lines are the true cluster parameter values as given in Tab. 1 and the red vertical lines are the mean of the probability distributions of the parameters.

The sampling parameters in our Bayesian analysis are $\Theta_c \equiv (x_c, y_c, M_{\text{tot}}(r_{200}), f_g(r_{200}), z)$, where x_c and y_c are cluster projected position on the sky. We further assume that the priors on sampling parameters are separable (Feroz et al. 2009) such that

$$\pi(\Theta_c) = \pi(x_c) \pi(y_c) \pi(M_T(r_{200})) \pi(f_g(r_{200})) \pi(z). \quad (8)$$

We use Gaussian priors on cluster position parameters, centred on the pointing centre and with standard-deviation of 1 arcmin and adopt a δ function prior on redshift z . The prior on $M_{\text{tot}}(r_{200})$ is taken to be uniform in $\log M$ in the range $M_{\text{min}} = 10^{14} M_{\odot}$ to $M_{\text{max}} = 6 \times 10^{15} M_{\odot}$ and the prior of $f_{\text{gas}}(r_{200})$ is set to be a Gaussian centred at the $f_{\text{gas}} = 0.13$ with a width of 0.02 (Vikhlinin et al. 2005, 2006; Komatsu et al. 2011; Larson et al. 2011). It should be noted that for the two low mass clusters we set the minimum mass to $M_{\text{min}} = 0.4 \times 10^{14} M_{\odot}$ in the prior range. A summary of the priors and their ranges are presented in Tab. 2.

Further details of our Bayesian methodology, modelling in-

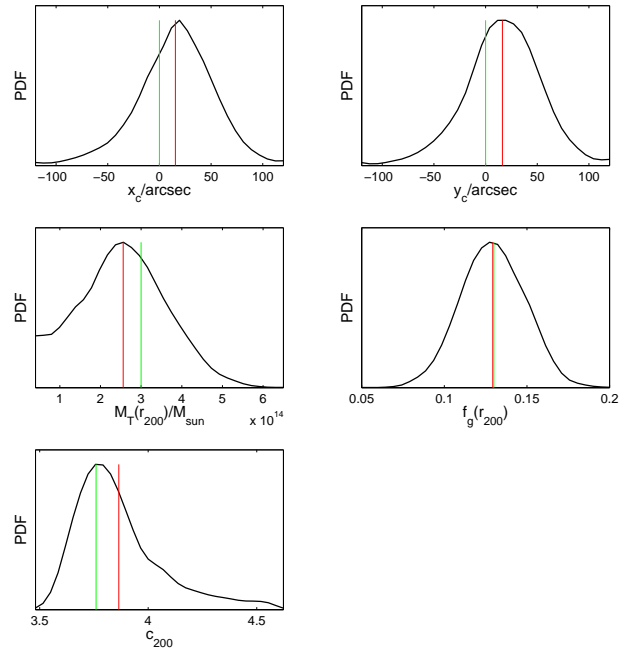


Figure 2. 1D marginalised posterior distributions of sampling parameters of clsim2 when c_{200} is calculated using equation (7). Green vertical lines are the true cluster parameter values as given in Tab. 1 and the red vertical lines are the mean of the probability distributions of the parameters.

Table 2. Summary of the priors on the sampling parameters. Note that $N(\mu, \sigma)$ represents a Gaussian probability distribution with mean μ and standard deviation of σ and $U(a, b)$ represents a uniform distribution between a and b .

Parameter	Prior
x_c, y_c	$N(0, 60)''$
$\log M_{\text{tot}}(r_{200})$	$U(14, 15.8) M_{\odot}$
$f_{\text{gas}}(r_{200})$	$N(0.13, 0.02)$

terferometric SZ data, primordial CMB anisotropies, and resolved and unresolved radio point-source models are given in Hobson & Masinger (2002), Feroz & Hobson (2008) and Feroz et al. (2009), AMI Consortium: Davies et al. (2011) and AMI Consortium: Olamaie et al. (2012).

3 RESULTS AND DISCUSSION

Fig. 1 shows 1D marginalised posterior distributions of sampling parameters for clsim2 (one of the lowest mass clusters) when c_{200} is also assumed to be a sampling parameter, (Olamaie et al. 2012).

The green vertical lines are the true values of the simulated cluster parameters while the red vertical lines represent the mean values of the probability distributions. It should be pointed out that similar results are obtained for all clusters in our sample. This results show that while this form of the parameterization can constrain cluster projected position on the sky and $M_{\text{tot}}(r_{200})$, the halo concentration parameter, c_{200} , is unconstrained and its mean value is just the mean of the prior range which suggests that the mean value of the distribution is strongly driven by the prior. This result, as we have seen in our previous studies of clusters of galaxies (AMI Consortium: Olamaie et al. 2012), also suggests a correlation between c_{200} and

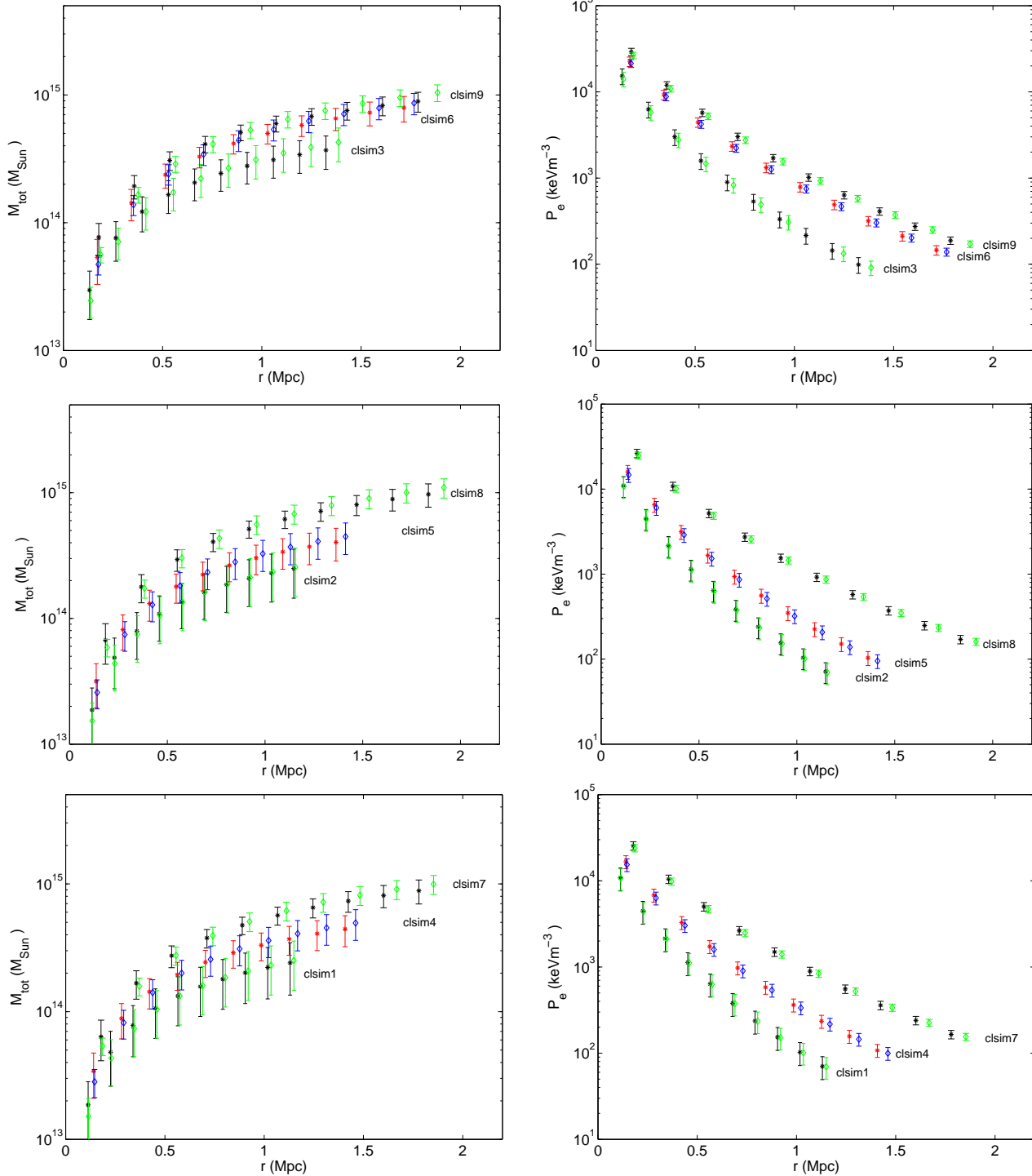


Figure 3. Integrated mass (*left*) and pressure (*right*) profiles as a function of r for nine simulated SZ clusters. In each panel, the plots with $*$ show the profiles when c_{200} is assumed as an input (sampling) parameter and the plots with \diamond show the profiles when c_{200} is calculated using equation (7).

the other two physical sampling parameters, i.e. $M_{\text{tot}}(r_{200})$ and z . The existence of such a correlation means that the analysis may result in a biased estimate of cluster parameters if it is not considered in the analysis.

Fig. 2 shows 1D marginalised posterior distributions of sampling parameters for clsim2 when we take into account the dependency of halo concentration on both the formation time and the dynamical state of the halo using equation (7). From the results it

is clear that this form of the parameterization can constrain c_{200} as well as other cluster parameters. Moreover, while NFW profiles are usually fitted using the two parameters R_s and c_{200} this parameterisation makes the profile a one-parameter profile. We notice that similar results were obtained upon analysing all the clusters in our sample. We also note that $f_{\frac{1}{2}}(r_{200})$ is hardly constrained in both parameterisations indicating that the gas fraction can not be constrained using SZ only data.

The *left* panel in fig. 3 presents the integrated mass profiles for our sample of nine SZ simulated galaxy clusters and the *right* panel shows the pressure profiles of these clusters. In each panel we have plotted the profiles out to r_{200} using the two forms of parameterizations: (1) assuming c_{200} as an input parameter in the analysis (*) and (2) calculating c_{200} using equation (7), (\diamond).

From the plots, the difference in estimating the cluster mass and its gas pressure using two forms of parameterizations is clear and becomes more significant as $M_{\text{tot}}(r_{200})$ increases. Our resulting constraints on c_{200} indicate that because this parameter is completely unconstrained when assumed as a sampling parameter, its best fit value is always the mean of the assumed prior range. This strong dependency on the prior range may indeed lead to a biased estimate of the cluster parameters including its mass.

4 CONCLUSION

We have studied the recovery of $M_{\text{tot}}(r)$ and $P_e(r)$ from the SZ effect for a sample of nine simulated galaxy clusters ($2.0 \times 10^{14} M_{\odot} < M_{\text{tot}}(r_{200}) < 1.0 \times 10^{15} M_{\odot}$) using the model described in Olamaie et al. (2012). This is motivated by the fact that SZ surface brightness is proportional to the line of sight integral of the ICM plasma so that SZ data can potentially constrain the cluster total mass.

To obtain an unbiased mass estimate we have carried out a detailed analysis of a series of simulated clusters using two different parameterizations within our model and its corresponding assumptions (Olamaie et al. 2012). In the first parameterization we assume that the halo concentration parameter c_{200} is also a sampling parameter. However, the results of the analysis show that the simulated SZ data can not constrain this parameter and therefore its mean value is driven by the prior range which may introduce biases in the ultimate cluster mass estimate. This results also suggests that c_{200} depends on the other model parameters.

In the second parameterization we consider the correlation of c_{200} with $M_{\text{tot}}(r_{200})$ and z within Λ CDM Universe (equation 7) as higher mass halos that are forming today are less concentrated than halos of lower mass that built up at an earlier epoch, where the mean density was higher. This parameterization clearly constrains c_{200} as AMI SZ data can constrain $M_{\text{tot}}(r_{200})$. We hence conclude that in order to obtain a robust estimate on cluster physical parameters including its mass it is crucial to consider the mass and redshift dependency of c_{200} as precisely as possible.

ACKNOWLEDGMENTS

The authors thank their colleagues in the AMI Consortium for numerous illuminating discussions regarding the modelling of galaxy clusters. The data analyses were carried out on the COSMOS UK National Supercomputer at DAMTP, University of Cambridge and we are grateful to Andrey Kaliazin for his computing assistance. MO acknowledges an STFC studentship.

REFERENCES

AMI Consortium: Davies et al., 2011, MNRAS, 415, 2708
 AMI Consortium: Olamaie M. et al., 2012, MNRAS, 419, 2921
 AMI Consortium: Zwart J. T. L., et al., 2008, MNRAS, 391, 1545
 Arnaud M., Pratt G. W., Piffaretti R., Böhringer H., Croston J. H., Pointecouteau E., 2010, A&A, 517, A92
 Bartlett J. G., Silk J., 1994, ApJ, 423, 12

Bhattacharya S., Habib S., Heitmann K., 2011, arXiv:1112.5479
 Birkinshaw M., 1999, PhR, 310, 97
 Bullock J. S., Kolatt T. S., Sigad Y., Somerville R. S., Kravtsov A. V., Klypin A. A., Primack J. R., Dekel A., 2001, MNRAS, 321, 559
 Buote D. A., Gastaldello F., Humphrey P. J., Zappacosta L., Bullock J. S., Brighenti F., Mathews W. G., 2007, ApJ, 664, 123
 Carlstrom J. E., Holder G. P., Reese E. D., 2002, ARA &A, 40, 643
 Challinor A., Lasenby A., 1998, ApJ, 499, 1
 Comerford J. M., Natarajan P., 2007, MNRAS, 379, 190
 Corless V. L., King L. J., Clowe D., 2009, MNRAS, 393, 1235
 Duffy A. R., Schaye J., Kay S. T., Dalla Vecchia C., 2008, MNRAS, 390, L64
 Eke V. R., Navarro J. F., Steinmetz M., 2001, ApJ, 554, 114
 Etti S., Gastaldello F., Leccardi A., Molendi S., Rossetti M., Buote D., Meneghetti M., 2011, A&A, 526, 1
 Feroz F., Hobson M. P., 2008, MNRAS, 384, 449
 Feroz F., Hobson M. P., Bridges M., 2009, MNRAS, 398, 1601
 Feroz F., Hobson M. P., Zwart J. T. L., Saunders R. D. E., Grainge K. J. B., 2009, MNRAS, 398, 2049
 Fixsen D. J., Cheng E. S., Gales J. M., Mather J. C., Shafer R. A., Wright E. L., 1996, ApJ, 473, 576
 Grainge K., Jones M. E., Pooley G., Saunders R., Edge A., Grainger W. F., Kneissl R., 2002, MNRAS, 333, 318
 Hobson M. P., Maisinger K., 2002, MNRAS, 334, 569
 Itoh N., Kohyama Y., Nozawa S., 1998, ApJ, 502, 7
 Komatsu E., et al., 2011, ApJS, 192, 18
 Larson D., et al., 2011, ApJS, 192, 16
 Macciò A. V., Dutton A. A., van den Bosch F. C., Moore B., Potter D., Stadel J., 2007, MNRAS, 378, 55
 Mandelbaum R., Seljak U., Hirata C. M., 2008, JCAP, 8, 6
 Muñoz-Cuartas J. C., Macciò A. V., Gottlöber S., Dutton A. A., 2011, MNRAS, 411, 584
 Nagai D., Kravtsov A. V., Vikhlinin A., 2007, ApJ, 668, 1
 Navarro J. F., Frenk C. S., White S. D. M., 1996, ApJ, 462, 563
 Navarro J. F., Frenk C. S., White S. D. M., 1997, ApJ, 490, 493
 Neto A. F., et al., 2007, MNRAS, 381, 1450
 Nozawa S., Itoh N., Kohyama Y., 1998, ApJ, 508, 17
 Olamaie M., Hobson M. P., Grainge K. J. B., 2011, arXiv:1109.2834
 Pointecouteau E., Giard M., Barret D., 1998, A&A, 336, 44
 Pointecouteau E., Arnaud M., Pratt G. W., 2005, A&A, 435, 1
 Rephaeli Y., 1995, ARA &A, 33, 541
 Rudd D. H., Zentner A. R., Kravtsov A. V., 2008, ApJ, 672, 19
 Salvador-Solé E., Manrique A., González-Casado G., Hansen S. H., 2007, ApJ, 666, 181
 Sunyaev R. A., Zeldovich Y. B., 1970, CoASP, 2, 66
 Vikhlinin A., Markevitch M., Murray S. S., Jones C., Forman W., Van Speybroeck L., 2005, ApJ, 628, 655
 Vikhlinin A., Kravtsov A., Forman W., Jones C., Markevitch M., Murray S. S., Van Speybroeck L., 2006, ApJ, 640, 691